Genomics and Proteomics:

Determination of an Angiotensin II-regulated Proteome in Primary Human Kidney Cells by Stable Isotope Labeling of Amino Acids in Cell Culture (SILAC)

Ana Konvalinka, Joyce Zhou, Apostolos Dimitromanolakis, Andrei P. Drabovich, Fei Fang, Susan Gurley, Thomas Coffman, Rohan John, Shao-Ling Zhang, Eleftherios P. Diamandis and James W. Scholey

J. Biol. Chem. 2013, 288:24834-24847.
doi: 10.1074/jbc.M113.485326 originally published online July 11, 2013

THE JOURNAL OF BIOLOGICAL CHEMISTRY VOL. 288, NO. 34, pp. 24834–24847, August 23, 2013
Published in the U.S.A.

Determination of an Angiotensin II-regulated Proteome in Primary Human Kidney Cells by Stable Isotope Labeling of Amino Acids in Cell Culture (SILAC)[S]

Received for publication, May 14, 2013, and in revised form, June 21, 2013 Published, JBC Papers in Press, July 11, 2013, DOI 10.1074/jbc.M113.485326

Ana Konvalinka[‡§1,2], Joyce Zhou[‡], Apostolos Dimitromanolakis[¶‖], Andrei P. Drabovich[¶‖], Fei Fang[‡], Susan Gurley[**], Thomas Coffman[**], Rohan John[¶], Shao-Ling Zhang[‡‡], Eleftherios P. Diamandis[¶‖3], and James W. Scholey[‡§2,3]

From the [‡]Institute of Medical Sciences, University of Toronto, Toronto, Ontario M5S 1A8, Canada, the [§]Division of Nephrology, Department of Medicine, University Health Network, University of Toronto, Toronto, Ontario M5G 2C4, Canada, the [¶]Department of Pathology and Laboratory Medicine, University of Toronto, Toronto, Ontario M5G 2C4, Canada, the [‖]Samuel Lunenfeld Research Institute, Mount Sinai Hospital, Toronto, Ontario M5G 1W7, Canada, the [**]Division of Nephrology, Department of Medicine, Duke University and Durham Veterans Affairs Medical Centers, Durham, North Carolina 27710, and the [‡‡]*Faculty of Medicine, Hôtel-Dieu Hôpital, University of Montreal, Montreal, Quebec H2W 1T8, Canada*

Background: Specific markers of kidney angiotensin-II (AngII) activity are needed.
Results: Eighteen AngII-regulated proteins were discovered and confirmed by proteomics in human kidney cells, whereas heme oxygenase-1 was validated in a mouse.
Conclusion: Heme oxygenase-1 and other AngII-regulated proteins represent novel markers of AngII activity.
Significance: AngII-regulated proteins may represent kidney-specific AngII activity markers in patients and in experimental models.

Angiotensin II (AngII), the major effector of the renin-angiotensin system, mediates kidney disease progression by signaling through the AT-1 receptor (AT-1R), but there are no specific measures of renal AngII activity. Accordingly, we sought to define an AngII-regulated proteome in primary human proximal tubular cells (PTEC) to identify potential AngII activity markers in the kidney. We utilized stable isotope labeling with amino acids (SILAC) in PTECs to compare proteomes of AngII-treated and control cells. Of the 4618 quantified proteins, 83 were differentially regulated. SILAC ratios for 18 candidates were confirmed by a different mass spectrometry technique called selected reaction monitoring. Both SILAC and selected reaction monitoring revealed heme oxygenase-1 (HO-1) as the most significantly up-regulated protein in response to AngII stimulation. AngII-dependent regulation of the HO-1 gene and protein was further verified in PTECs. To extend these *in vitro* observations, we overlaid a network of significantly enriched gene ontology terms from our AngII-regulated proteins with a dataset of differentially expressed kidney genes from AngII-treated wild type mice and AT-1R knock-out mice. Five gene ontology terms were enriched in both datasets and included HO-1. Furthermore, HO-1 kidney expression and urinary excretion were reduced in AngII-treated mice with PTEC-specific AT-1R deletion compared with AngII-treated wild-type mice, thus confirming AT-1R-mediated regulation of HO-1. Our *in vitro* approach identified novel molecular markers of AngII activity, and the animal studies demonstrated that these markers are relevant *in vivo*. These interesting proteins hold promise as specific markers of renal AngII activity in patients and in experimental models.

There is evidence that both diabetic and nondiabetic chronic kidney diseases (CKD)[4] result in activation of the renin-angiotensin system (RAS) (1, 2). The mainstay of current CKD therapy focuses on blockade of the RAS, which has been demonstrated to slow down CKD progression (3–6). However, apart from reducing blood pressure to target levels, there is no specific guideline for the extent of RAS blockade in patients with CKD. This is problematic because some clinical studies suggest that more aggressive or dual RAS blockade may be beneficial in proteinuric CKD, independent of blood pressure (7–9), even though the choice of agents and dosing remains uncertain. Recently, enthusiasm for dual RAS blockade has been tempered by reports of adverse events when dual blockade is applied broadly to patients with CKD (10, 11). All this comes on the background of having no measure of RAS bioactivity in the kidney.

The principal effector molecule of RAS is angiotensin II (AngII). AngII is an octapeptide generated by angiotensin-converting enzyme cleavage of a decapeptide angiotensin I (AngI). AngI is initially formed by renin-mediated cleavage of angio-

[S] This article contains supplemental Tables S1–S3.
The mass spectrometry SILAC data have been deposited in the ProteomeXchange Consortium (http://proteomecentral.proteomexchange.org) via the PRIDE partner repository (91) with the dataset identifier PXD000183.

[1] Recipient of a fellowship grant from the Kidney Foundation of Canada. To whom correspondence should be addressed: Division of Nephrology, Toronto General Hospital, University Health Network, 8N-859, 200 Elizabeth St., Toronto, Ontario M5G 2C4, Canada. Tel.: 416-586-4800 (Ext. 2968); Fax: 416-340-4999; E-mail: ana.konvalinka@mail.utoronto.ca.
[2] Supported by operating grants from the Kidney Foundation of Canada and from the AMGEN Canada Investigator Sponsored Initiative Research Program.
[3] Both authors contributed equally to this work.

[4] The abbreviations used are: CKD, chronic kidney disease; AngII, angiotensin II; AT-1R, angiotensin II type 1 receptor; EM, enrichment map; ER, endoplasmic reticulum; GO, gene ontology; HO-1, heme oxygenase 1, decycling; Nrf2, nuclear factor (erythroid derived-2)-like 2; PDCD4, neoplastic transformation inhibitor; PTEC, proximal tubular epithelial cell; PTKO, proximal tubule-specific knock-out; qRT-PCR, quantitative RT-PCR; RAS, renin angiotensin system; SILAC, stable isotope labeling with amino acids in cell culture; SRM, selected reaction monitoring; SSB, La autoantigen; FDR, false discovery rate; H, heavy; L, light; Th, Thompson.

tensinogen, a 53-kDa protein constitutively secreted into the circulation by the liver. AngII has long been known to be a potent vasoconstrictor (12, 13) that can also increase sodium and water reabsorption along the nephron, as well as lead to secretion of aldosterone from the adrenal gland and activation of the sympathetic nervous system. AngII has thus been implicated in an increase in systemic blood pressure and extracellular fluid volume. In addition to systemic hemodynamic effects, AngII influences renal hemodynamics and glomerular filtration rate. It causes vasoconstriction of glomerular arterioles through the release of thromboxane A2 (14).

It has been recognized that in addition to the circulating systemic RAS, local RAS exists in several major organs, including the kidney, heart, brain, adrenal gland, and vascular endothelium (15–19). This tissue-specific activation of RAS can be disconnected from the systemic RAS, as evidenced by 1000 times higher levels of AngII in the peritubular capillary and the proximal tubule compared with the circulating AngII levels (20). AngII is thus an endocrine, paracrine, and intracrine factor.

AngII exerts multiple adverse hemodynamic and nonhemodynamic effects on renal cells that are mediated by AT-1R. Some of the nonhemodynamic effects include inflammatory cell infiltration, oxidative stress, and renal fibrosis. It has been demonstrated that intra-renal AngII may be more important for progression of renal injury than systemic AngII (21–24). Indirect evidence suggests that PTECs are sites of intra-renal AngII accumulation (25, 26), and recent *in vivo* studies identified the PTEC as a key site in blood pressure regulation by AngII (27). Additionally, AngII leads to PTEC growth, differentiation, and sodium retention (28). The function of PTECs is regulated by both circulating and locally formed AngII (29, 30). All major components of RAS have been demonstrated in PTECs (31–34). AT-1R is highly expressed in PTECs and acts as the main signaling receptor of AngII. In clinical histopathology, tubular atrophy and interstitial fibrosis are the hallmarks of progression of all CKDs, implicating these cells in the pathophysiology leading to end stage renal disease. Finally, PTECs communicate directly with urine *in vivo* and secrete potentially important proteins that could be detected by examining this biofluid.

The aim of this study was to identify novel proteins that reflect PTEC response to AngII. We identified the proteome of primary human PTECs after exposure to AngII, and we compared it with nontreated PTECs by using stable isotope labeling of amino acids in cell culture (SILAC). This enabled us to define AngII-regulated proteins. We then verified candidates by a combination of quantitative (qRT)-PCR, ELISA, and selected reaction monitoring (SRM). We also performed bioinformatics-based and *in vivo* validation of our main findings in mice treated with AngII.

EXPERIMENTAL PROCEDURES

Cell Culture—Primary human renal PTECs were purchased from Lonza Walkersville Inc. These cells originated from three different individuals from different age groups, both male and female. They were cultured in custom-made Dulbecco's modified Eagle's medium (DMEM), free of arginine and lysine (AthenaES), and supplemented with 10% v/v dialyzed fetal bovine serum, 10 ng/ml EGF, 5 μg/ml transferrin, 5 μg/ml insulin, 0.05 μM hydrocortisone, 50 units/ml penicillin, and 50 μg/ml streptomycin. Heavy arginine ($^{13}C_6$) and heavy lysine ($^{13}C_6{}^{15}N_2$) were added to DMEM "heavy" bottles used to incubate heavy (H)-labeled cells, whereas light arginine ($^{12}C_6$) and lysine ($^{12}C_6{}^{14}N_2$) were added to "light" DMEM used to incubate light (L)-labeled cells, as described previously (35). Cells were divided into two populations (H and L), and incubated in their respective media for six doubling times until passage 6. Once labeled, cells were grown in T75 flasks to ~80% confluence. They were then serum-deprived for 18 h and subjected to 10^{-7} M (final concentration) AngII or control (medium alone). Following stimulation, PTECs were incubated for 8 h. Conditioned medium (supernatant) representing the cellular secretome was collected and stored at −80 °C. Cells were then washed three times with PBS, harvested with trypsin, and snap-frozen at −80 °C until further analysis. All cells were cultured in a humidified incubator at 37 °C and 5% CO_2. All media were freshly made and filtered using a 0.22-μm syringe filter.

PTECs used for Western blotting, qRT-PCR, and ELISA experiments were grown in DMEM with a glucose concentration of 4.5 g/liter (Invitrogen). The medium was enriched with 10% v/v fetal bovine serum (FBS), and cells were otherwise treated the same as in SILAC experiments.

Proteomic Studies of SILAC-labeled PTECs Using Two-dimensional LC-MS/MS—Cell pellets were thawed on ice, resuspended in 200 μl of 0.2% w/v acid-labile detergent RapiGest SF (sodium-3-[(2-methyl-2-undecyl-1,3-dioxolan-4-yl)-methoxyl]-1-propanesulfonate, Waters, Milford, MA) in 25 mM ammonium bicarbonate, vortexed, and sonicated three times for 30 s. All lysates were centrifuged for 20 min at 15,000 rpm at 4 °C. Total protein concentration was measured using a Coomassie (Bradford) protein assay reagent (Pierce). H and L samples were mixed in a 1:1 total protein ratio. Proteins in detergent solution were denatured at 60 °C, and the disulfide bonds were reduced with 10 mM dithiothreitol. Following reduction, the samples were alkylated with 20 mM iodoacetamide. Samples were then digested overnight at 37 °C with sequencing grade modified trypsin (Promega, Madison WI). A trypsin/total protein ratio of 1:50 was used. The supernatants were dialyzed in 1 mM ammonium bicarbonate with two buffer exchanges, using a molecular cutoff of 3.5 kDa, for 24 h. They were subsequently lyophilized, and a similar procedure as for the analysis of lysates was followed. After digestion, RapiGest SF detergent was cleaved with trifluoroacetic acid, 1% v/v final concentration, and samples were centrifuged at 4,000 rpm. Upon removal of Rapigest, tryptic peptides were diluted to 500 μl with SCX mobile phase A (0.26 M formic acid in 5% v/v acetonitrile; pH 2–3) and loaded directly onto a 500-μl loop connected to a PolySULFOETHYL A™ column (2.1-mm inner diameter × 200 mm, 5 μm, 200 Å, The Nest Group Inc.). The SCX chromatography and fractionation were performed on an HPLC system (Agilent 1100) using a 60-min two-step gradient. An elution buffer that contained all components of mobile phase A with the addition of 1 M ammonium formate was introduced at 10 min and increased to 20% at 30 min and then to 100% at 45 min. Fractions were collected every 1 min from the 20-min time point onward. The resulting 20 fractions (200 μl each) corresponding to chromatographic peaks of eluting peptides were collected. Peptides in each fraction were identified by

LC-MS/MS as described previously (36). Briefly, peptides were extracted with 10 μl of OMIX C18 MB tips (Varian, Lake Forest, CA), eluted in 5 μl of 65% v/v acetonitrile, diluted to 85 μl with 0.1% v/v formic acid in pure water, and loaded onto a 3-cm C18 trap column (with an inner diameter of 150 μm; New Objective), packed in-house with a 5-μm Pursuit C18 (Varian). Eluted peptides from the trap column were subsequently loaded onto a resolving analytical PicoTip Emitter column, 5 cm in length (with an inner diameter of 75 μm and 8 μm tip, New Objective) and packed in-house with 3 μm Pursuit C18 (Varian, Lake Forest, CA). The trap and analytical columns were operated on the EASY-nLC system (Thermo Fisher Scientific, San Jose, CA), and this liquid chromatography setup was coupled on line to an LTQ-Orbitrap XL hybrid mass spectrometer (Thermo Fisher Scientific, San Jose, CA) using a nano-ESI source (Proxeon Biosystems, Odense, Denmark). Each fraction was run using a 90-min gradient, in duplicate, and analyzed in a data-dependent mode in which a full MS1 scan acquisition from 450 to 1450 m/z in the Orbitrap mass analyzer (resolution 60,000) was followed by MS2 scan acquisition of the top six parent ions in the linear ion trap mass analyzer. The following parameters were enabled: monoisotopic precursor selection, charge state screening, and dynamic exclusion. In addition, charge states of +1, >4, and unassigned charge states were not subjected to MS2 fragmentation. For protein identification and data analysis, Xcalibur software (version 2.0.5; Thermo Fisher) was utilized to generate RAW files of each MS run.

Data Analysis—The resulting raw mass spectra from each pooled fraction were analyzed using Andromeda search engine (MaxQuant software version 1.2.2.2) (37), on the nonredundant IPI human database version 3.62. The raw files from all biological replicates were analyzed simultaneously with MaxQuant. To assess the false-positive rate, a reverse hit database was created by MaxQuant. A false discovery rate (FDR) of 1% was specified. Up to two missed cleaves were allowed, and searches were performed with fixed carbamidomethylation of cysteines, variable oxidation of methionine residues, and N-terminal acetylation. Arg (+6 Da) and Lys (+8 Da) heavy labels were selected. A fragment tolerance of 0.5 Da and a parent tolerance of 20 Da were used, with trypsin as the digestion enzyme. Re-quantification and matching between runs was selected. Protein was identified with a minimum of one unique peptide. Quantification was performed using unmodified unique and razor peptides and a minimum of one counted ratio. The median normalized protein ratios of biological replicates were used for further analyses. Perseus software (version 1.2.0.17) was used to calculate significance A. Lysate experiments were further analyzed to select differentially regulated proteins, as the supernatant yielded 3–4 times fewer protein identifications. Protein was considered to be significantly differentially regulated if its ratio was significant by significance A with $p < 0.01$ in $\geq 2/4$ experiments. FDR for proteins calculated with these parameters was 0.0006. This threshold was selected because at this level of significance, and taking into account the total number of proteins (4618), less than three proteins should have been found by chance alone. Proteins that had ratios changing significantly in opposite directions in any of the replicates were eliminated. Additionally, proteins were eliminated if their ratios were above two standard deviations from the mean in the control experiment, where no treatment was applied to either the H or L sample. Individual peptide ratios for all differentially regulated candidates were examined manually. If ratios of proteotypic (unique) peptides of the same protein were changing significantly in opposite directions, or if posterior error probability of peptides was >0.05, these proteins were not pursued further by SRM. The final list for development of SRM methods included 51 proteins.

SRM—SRM methods were developed for confirmation of protein ratios in cell lysates. SRM is a quantitative analytical assay performed with a triple quadrupole mass spectrometer. It can be used for relative or absolute quantification. Assumption is made that the amount of measured proteotypic (unique) peptide represents the amount of the protein of interest. An SRM assay includes the following steps: sample preparation and digestion of proteins in the biological fluid, liquid chromatography (LC) separation of peptides, ionization of peptides with nanoelectrospray ionization (nano-ESI), filtering of peptides of interest in the first quadrupole (Q1), fragmentation of peptides in the second quadrupole (Q2), filtering of peptide fragments in the third quadrupole (Q3), measurement of several fragment ion intensities, and integration of the ion signals. With state-of-the-art SRM assays, up to 100 peptides representing 100 medium-to-high abundance proteins (10 ng/ml to 1 mg/ml) can be measured simultaneously in the unfractionated digest of proteins, while achieving coefficients of variation under 20%.

Initially, PTPAtlas of the Peptide Atlas was used to select the five most highly observable peptides for each of the top 51 proteins based on the occurrence of +2 ions. Fully tryptic and doubly charged peptides with 7–20 amino acids were chosen. Peptides with methionine, tryptophan, and N-terminal cysteine residues were avoided, whenever possible. All peptides were also analyzed with the Basic Local Alignment Search Tool (BLAST) to ensure that peptides were unique to each protein. A list of 194 peptides corresponding to the top 41 proteins (the remaining 10 proteins were not readily amenable to SRM) was uploaded to Skyline software (38) and was used to design *in silico* survey SRM methods. Transitions containing y ions from y+3 to last ion-1 for both heavy and light peptides were selected (~7 light and 7 heavy transitions per peptide). In addition, nine intense peptides from six high abundance proteins that our group had previously monitored were included to serve as internal loading controls. An equimolar mixture of light and heavy SILAC-labeled PTECs (L-[$^{13}C_6$,$^{15}N_2$]lysine, +8 Da, and L-[$^{13}C_6$]arginine, +6 Da) was used to experimentally test 2645 transitions. In the first step of method development, 9–10 peptides and about 100 transitions were included in each survey SRM method and run in a nonscheduled mode with a 20-ms scan time per transition on a 60-min gradient. Q1 was set to 0.2 Thompson (Th) and Q3 to 0.7 Th. Given the low abundance nature of most candidate proteins, and the difficulty in finding peaks in nonscheduled SRM methods, we pursued 18 proteins only. Additionally, the two most consistently observed high abundance peptides with congruent H/L ratios (SYELPDGQVITIGNER peptide of β-actin, and INVYYNEATGGK peptide of tubulin β-4B chain) were monitored as internal controls. Nine high abundance peptides all had similar ratios. Thus,

in the second step, three peptides and under 50 transitions were included in each of 10 survey SRM methods and run in a non-scheduled mode with 20-ms scans per transition. Q1 was set to 0.4 Th and Q3 to 0.7 Th. We looked for co-elution of all light and all heavy transitions for each peptide. Retention times, relative intensities of peptides, and the three most intense transitions per peptide were recorded (supplemental Table S1). Transitions with fragment m/z higher than precursor m/z were preferable, but transitions with lower m/z were not excluded if they had high intensity (especially at proline residue). As a reference to exclude possible interferences, we used the SRM signal of SILAC-labeled heavy cells.

Peptides were separated by a 60-min C18 reversed phase liquid chromatography (EASY-nLC, Proxeon, Odense, Denmark) and analyzed by a triple-quadrupole mass spectrometer (TSQ Vantage, Thermo Fisher Scientific Inc., San Jose, CA) using a nanoelectrospray ionization source, as described previously (39–41). Reproducibility of SRM signal was ensured by running a quality control solution of 0.1 fmol/μl BSA every 5 runs. Raw files recorded for each sample were analyzed using Pinpoint software (Thermo Fisher Scientific Inc., San Jose, CA), and CSV files with peptide areas were extracted. Pinpoint was used for identification and visualization of transitions, as well as manual verification of co-elution of heavy and light transitions. Skyline was subsequently used for reporting of peptide ratios. Pinpoint and Skyline ratios were concordant. Peptide H/L ratios extracted from Skyline were divided by the H/L ratio of internal standards (to control for the differences in mixing). Protein ratios were calculated as an average of all peptide ratios for each protein (supplemental Table S2). If different peptides from the same protein had distinctly different intensities, only the highest intensity peptide was included in the calculation. Collision energy (CE) was calculated in Skyline by using the following equation: CE = 0.03 × (precursor m/z) + 2.905 (42).

Bioinformatic Analyses—Proteins that had H/L ratios of >1.2 or <0.8 (which was ≥2 standard deviations from the mean) in any one biological replicate were included in the enrichment analysis. BiNGO plugin (43) was used to perform the enrichment analysis. Full GO was used as a reference set. Enriched GO terms were then visualized using EM plugin in Cytoscape (version 2.8.2) (44). Gene sets, such as pathways and Gene Ontology terms, are organized into a network called the "enrichment map." In this way, mutually overlapping gene sets cluster together, making interpretation easier. Ingenuity pathway analysis (Ingenuity® Systems) was used to define overrepresented pathways and interaction networks.

Western Blot—A subpopulation of labeled SILAC cells was separated into a 6-well plate with each experiment conducted. These cells were serum-deprived for 18 h and then stimulated with control media or sequentially with 20 μM Losartan for 30 min, and/or AngII (10^{-7} M) for 5 min. Western blotting was performed for phosphorylated ERK and total ERK as described previously (45). The primary antibodies against p44/42 ERK and total 44/42 ERK were polyclonal and developed in rabbit (Cell Signaling). The secondary antibody was anti-rabbit antibody developed in goat (Santa Cruz Biotechnology). Mouse kidney Western blotting with HO-1 antibody (Abcam 13243) was performed on fresh frozen kidney tissues. Tissue proteins were solubilized in modified RIPA buffer (150 mM sodium chloride, 50 mM Tris-HCl (pH 7.4), 1 mM EDTA, 1% v/v Triton X-100, 1% w/v sodium deoxycholic acid, 0.1% v/v SDS) followed by sonication. Total protein was then extracted from supernatant, after centrifugation.

qRT-PCR—Total RNA was extracted from cultured primary PTECs using a kit (RNeasy Mini; Qiagen Canada, Mississauga, Ontario, Canada). RNA was then reverse-transcribed into first strand complementary DNA (cDNA). mRNA expression levels for *HMOX1* (Hs01110250_m1), *TXNIP* (Hs00197750_m1), and *DNAJB4* (Hs00199826_m1) were quantified by real time PCR (TaqMan) using a sequence detection system (ABI Prism 7900; Applied Biosystems, Foster City, CA) as described previously (46). *GAPDH* (4352934E) was used as internal control. Specific human primer sets were purchased from Applied Biosystems (Foster City, CA).

Enzyme-linked Immunosorbent Assay (ELISA)—Total HO-1 human ELISA DuoSet (R&D Systems DYC3776) was used to assay PTEC HO-1 protein expression. HO-1 protein measurements were adjusted for total protein concentration. To minimize inter-plate variation, HO-1 protein measurements were expressed as ratio of AngII-to-control for each plate. Mouse HO-1 ELISA kit (USCN Life Science Inc. E90584Mu) was used to measure urine HO-1 protein levels. Urine samples were prepared and assayed as per manufacturer's instructions. Urine creatinine was measured by the Jaffé colorimetric method (47).

Experimental Animals—Mice with a conditional *Agtr1a* allele were generated as described previously (27, 48). Briefly, a targeting vector was generated containing a *PGK-Neo* cassette for positive selection with *loxp* sites engineered in positions flanking exon 3 of the *Agtr1a* gene. Correctly targeted 129 ES cell clones were identified by Southern analysis, and the *PGK-Neo* cassette was removed by transient transfection with *Flp* recombinase. In the presence of Cre recombinase, a null allele was generated. Appropriately modified ES cell lines were expanded and injected into blastocysts to generate chimeras. Germ line transmitting chimeras were bred with wild-type 129/SvEv mice (Taconic Farms) to generate inbred 129/SvEv $Agtr1a^{flox/+}$ mice. The *Pepck-Cre* transgene was back-crossed more than 10 generations onto the 129/SvEv background, and these 129/SvEv PEPCK Cre mice were bred with 129/SvEv $Agtr1a^{flox/flox}$ mice to generate proximal tubule knock out (PTKO) mice. The pattern of transgene expression in the proximal tubule was verified by inter-crossing with the *ROSA26R* reporter line. *Agtr1a* gene expression, quantified using qRT-PCR, was reduced by 45% in $Cre{+}Agtr1a^{flox/flox}$ (PTKO) mice compared with $Cre\text{-}Agtr1a^{flox/flox}$ controls ($p = 0.01$). To confirm deletion of AT-1A receptor protein, specific binding of ^{125}I-[Sar1,Ile8]AngII was examined using quantitative autoradiography. Nonglomerular AT1-specific ^{125}I-AngII renal cortical binding was markedly reduced by ≈40% in kidneys from PTKO mice compared with controls, whereas the extent of glomerular binding was virtually identical between the groups. PTKO and other mice were bred and maintained in the animal facility at the Durham Veterans Affairs Medical Center according to National Institutes of Health guidelines.

One mouse from the PTKO group was excluded from analyses because it had the smallest kidneys and the highest levels of

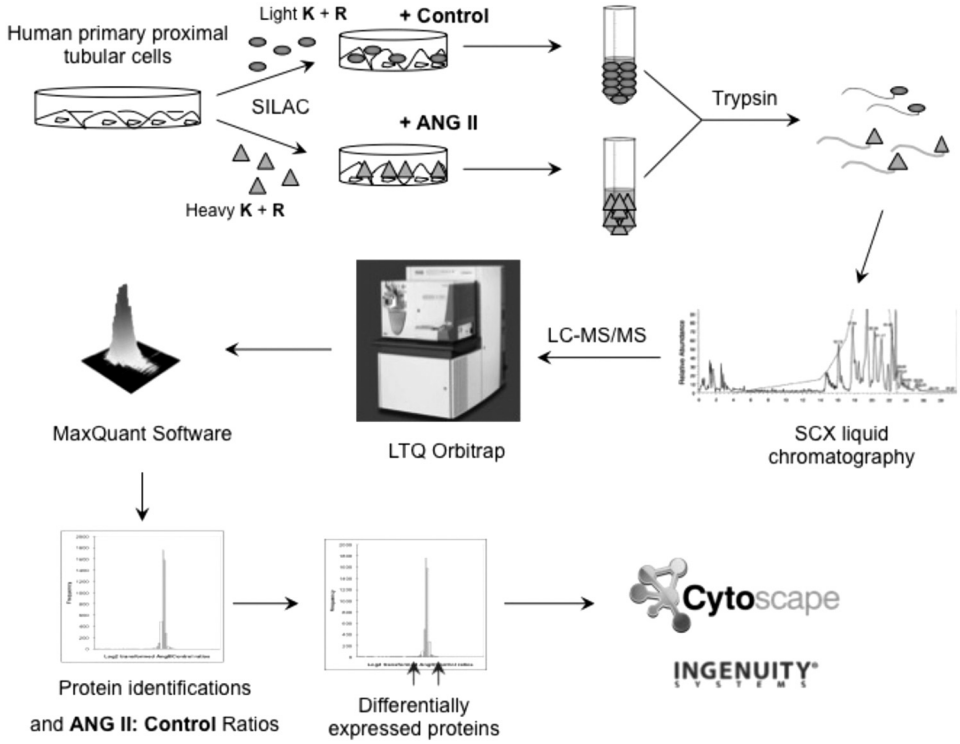

FIGURE 1. **Experimental scheme.** The figure demonstrates a simplified experimental flow, including SILAC labeling, cell treatment, protein digestion, HPLC followed by LC-MS/MS, data analysis by MaxQuant, assignment of AngII/control protein ratios, selection of differentially regulated proteins, and bioinformatic analyses by Cytoscape and Ingenuity Pathway Analysis.

urine and tissue HO-1 expression meeting the criteria of an outlier, by Dixon's *Q*-test at $\alpha = 0.05$. We concluded that this mouse was sick due to factors unrelated to genetic manipulation or treatment.

Angiotensin II Infusion—Angiotensin II (Sigma A9525) was dissolved in sterile saline (0.9% NaCl) and infused via osmotic minipump for 15 days at 1000 ng/kg/min. Animals were sacrificed, and kidneys were harvested, weighed, decapsulated, and immediately frozen in liquid nitrogen. A 24-h urine collection was performed at day 13 during AngII infusion. Urine samples were stored at −80 °C.

Immunohistochemistry—Fresh frozen mouse kidneys were cut into sections and stained with HO-1 polyclonal antibody (StressGen Assay, Cedarlane Corp. SPA-895-D). Immunohistochemistry protocol followed ABC kit SC-2018 from Santa Cruz Biotechnology.

Statistical Analyses—All values are reported as mean ± S.E., unless stated otherwise. Statistical comparison between experimental groups was performed using a two-tailed Student's *t* test. *p* values <0.05 were considered statistically significant, unless stated otherwise. Perseus software (version 1.2.0.17) was used for calculation of significance of protein ratios. Benjamini Hochberg correction for multiple testing was applied. Statistical language R (version 2.13.1) was used for selection of candidates and for linear regression. GraphPad Prism 5 software was used for other statistical tests (GraphPad, La Jolla, CA).

RESULTS

SILAC—The experimental scheme is shown in Fig. 1. Briefly, PTECs at the 2nd passage were split into two populations and incubated in H or L SILAC media for six doubling times. They were then deprived of serum for 18 h, and subsequently H-labeled cells were stimulated with AngII (10^{-7} M) and L-labeled cells with untreated medium for 8 h. Cell lysates were collected and lysed as described under "Experimental Procedures." The experiment was repeated four times. In three experiments we added AngII to the H-labeled cells, and in one experiment we added AngII to the L-labeled cells (reverse labeling). We performed an additional experiment, in which AngII was added to the H-cells, and we only collected the supernatant. In the final experiment, we labeled cells as H and L but did not add AngII to either H or L cells for control purposes. In each set of labeling experiments, we determined that AngII led to phosphorylation of ERK, as explained below.

Control Experiments—Two control experiments were performed. When AngII engages the AT-1R, PTECs respond by activating a cascade of signaling events, one of which is phosphorylation of ERK. Western blot analysis showed that AngII led to AT-1R-dependent phosphorylation of ERK in comparison with the control cells (Fig. 2*A*). Although phosphorylation of ERK is one of many downstream events initiated by AngII, this was an important confirmation that PTECs exhibited a biological response to AngII. The second control experiment involved labeling PTECs with H and L media and comparing their proteomes, to ensure that the changes in proteome due to the conditioned media were not attributed to AngII stimulus. The distribution of log2 transformed H/L ratios of these proteins is demonstrated in Fig. 2*B*. Standard deviation (S.D.) of the transformed ratios was 0.33, and this was greater than in the

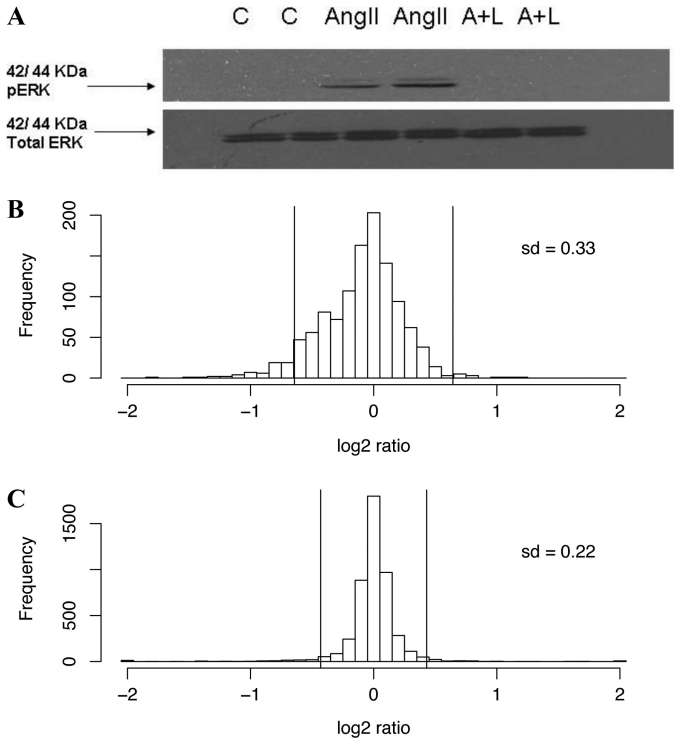

FIGURE 2. **Control experiments.** *A,* representative Western blot demonstrating phosphorylation of ERK after stimulation with AngII (which is AT-1 receptor-dependent) only in cells exposed to AngII, but not in those exposed to medium alone (C) or to AngII and AT-1 receptor blocker losartan (*A+L*). *B,* histogram of log2-transformed H/L ratios for labeled but unstimulated PTECs. *C,* histogram of log2-transformed AngII/control ratios in four lysate experiments. *Vertical lines* represent 1.96·S.D.

four stimulation experiments, as indicated below. This control experiment was thus underpowered for the purpose of determining variance in the stimulation experiments, although it was still suitable for identifying hypervariable outliers in the absence of stimulation. Hepatocyte nuclear factor 1-β was the only protein that had a H/L ratio more than two S.D. outside of the mean in the absence of AngII stimulation and that also subsequently appeared on the list of AngII-regulated proteins. Hepatocyte nuclear factor 1-β was thus eliminated from the final list of differentially regulated candidates.

AngII-induced Proteome in PTECs—We identified 5011 proteins and quantified 4975 in the four-cell lysate experiments together with one supernatant experiment (at 1.0% FDR). We then restricted our analyses to the four-cell lysate experiments. The distribution of normalized log2-transformed H/L ratios of these proteins is shown in Fig. 2*C*. S.D. of the transformed ratios was 0.22. 4618 proteins were quantified, and 83 of these proteins were differentially regulated by AngII, when applying the criteria described under "Experimental Procedures." Those AngII-regulated proteins that were confirmed by SRM are shown in Table 1. There were 53 up-regulated and 30 down-regulated proteins (supplemental Table S3). The most significant GO biological process enriched among these 83 proteins was apoptosis, and the most enriched cellular organelle was ER (Table 2). Biological processes linked to apoptosis were also significantly enriched in the analysis of AngII-regulated proteins from the supernatant (data not shown). The candidate with the most consistent and significant expression in all replicates was heme oxygenase 1 (HO-1), which was up-regulated in all experiments, including the supernatant. HO-1 is induced by oxidative stress and is a known target of nuclear factor (erythroid derived-2)-like 2 (Nrf2) transcription factor. Notably, there were three other proteins directly regulated by Nrf2 as follows: heat shock 40-kDa protein 1 homolog (49), thioredoxin-interacting protein (50), and ubiquitin-conjugating enzyme E2 R1. The direction of change in expression of these proteins would support increased Nrf2-mediated transcription. Another protein, La ribonucleoprotein domain family member 4, was significantly up-regulated following AngII stimulation. La autoantigen (SSB) can induce rapid Nrf2 translocation to the nucleus (51) and transcription of downstream genes. SSB appears to be a homolog of La ribonucleoprotein domain family member 4 based on sequence similarity (BLAST algorithm), functional similarity from distiller algorithm (both affect nuclear transcription), and co-expression.

SRM Confirms Differential AngII-mediated Protein Expression of Top Candidates—We next used SRM assays to confirm differential protein expression in response to AngII stimulation in PTECs. As explained under "Experimental Procedures," SRM is a mass spectrometry-based quantitative technique used for relative or absolute quantification. Assumption is made that the amount of measured proteotypic (unique) peptide represents the amount of the protein of interest. With the presence of both heavy-labeled and light-labeled proteotypic peptides, confident identification and quantification of peptides is enabled. SRM assays were developed for 18 candidate proteins. Proteins involved in processes deemed to be important by GO analyses, such as apoptosis, regulation of intracellular kinase activity, regulation of leukocyte migration, and transforming growth factor β binding, were selected. SILAC-labeled PTEC lysates were used to monitor co-eluting heavy and light peptide transitions of all 18 proteins. Heavy and light peak areas were used to calculate AngII-to-control ratios. These ratios were further adjusted by internal peptides, which served as loading controls. Peak areas of peptides of HO-1, neoplastic transformation inhibitor (PDCD4), thrombospondin-1, and Rho-related GTP-binding protein are demonstrated in Fig. 3. All 18 proteins demonstrated concordant ratios to SILAC experiments (Table 1). The supplemental Table S1 displays details of peptides monitored, transitions, retention times, and collision energies. We demonstrated using SRM that 18 of our candidates had concordant ratios to those obtained by SILAC, thus confirming their differential expression in PTECs upon AngII stimulation.

Bioinformatic Analyses—We aimed to better understand the networks and pathways associated with proteins differentially regulated by AngII. We hypothesized that even small changes in protein expression across a large number of proteins may lead to distinct physiological effects. We thus selected proteins with >20% change in expression upon stimulation with AngII (this was close to 2 S.D. from the mean). This list of proteins was analyzed using the Biological Networks Gene Ontology (BiNGO) plugin (43) of Cytoscape (44). Cytoscape is a bioinformatic software that allows complex network analysis and visualization. BiNGO plugin is a tool to determine enriched GO terms (biological processes, molecular functions, and cell compartments) in a set of genes or proteins. Using BiNGO, we

TABLE 1

Comparison of SILAC and SRM ratios for the proteins monitored

Protein	SILAC AngII/control ratio (median)	SRM AngII/control ratio (mean)
Heme oxygenase-1 (HO-1)	1.58	2.12
Neoplastic transformation inhibitor (PDCD4)	0.68	0.79
Retinol dehydrogenase 10 (RDH10)	1.70	1.50
Rho-related GTP-binding protein RhoB (RHOB)	0.74	0.69
Thioredoxin-interacting protein (TXNIP)	0.63	0.63
DnaJ homolog subfamily B member 4 (DNJB4)	1.27	1.40
ADP ribosylation factor-like protein 7 (ARL4C)	1.39	2.61
La ribonucleoprotein domain family member 4 (LARP4)	1.30	2.09
Protein EFR3 homolog A (EFR3A)	0.55	0.81
Guanine nucleotide exchange factor H1 (ARHGEF2)	1.23	1.13
3-Hydroxy-3-methylglutaryl-coenzyme A synthase (HMGCS1)	1.30	2.00
Apoptosis-associated nuclear protein (PHLDA1)	1.30	4.62
Deubiquitinating protein VCIP135 (VCPIP1)	1.40	1.17
Importin subunit α-2 (KPNA2)	1.22	1.27
Retinoic acid-induced protein 15 (SMYD5)	0.75	0.86
Thrombospondin-1 (TSP-1)	0.84	0.74
Transmembrane protein 41B (TMEM41B)	1.24	1.56
Cervical mucin-associated protein (DBNL)	1.28	1.21

TABLE 2

The most representative/informative GO terms among the 83 differentially regulated proteins

Corrected *p* value was obtained by applying Benjamini Hochberg correction for multiple testing. The whole annotation was used as a reference set. Statistical analysis was performed by BiNGO plugin of Cytoscape.

Gene ontology	*p* value	Corrected *p* value	Genes
Apoptosis	$7.16\ e^{-6}$	0.004	*ARGHEF2, JMJD6, THBS1, PDCD4, APIP, BAG1, PHLDA1, STK17A, TNFRSF10B, FAS, RPS6, RHOB*
Erythrocyte homeostasis	$6.56\ e^{-5}$	0.013	*LYN, JMJD6, HMOX1, RPS6*
Regulation of intracellular protein kinase cascade	$9.23\ e^{-5}$	0.015	*EGFR, HMOX1, LEPR, TNFRSF10B, LYN, THBS1, DBNL, PDCD4*
Positive regulation of signal transduction	$2.24\ e^{-4}$	0.024	*EGFR, HMOX1, LEPR, TNFRSF10B, ADA, LYN, THBS1*
Mitotic cell cycle	$2.80\ e^{-4}$	0.027	*EGFR, ARHGEF2, NDE1, ANAPC3, CDC34, VCPIP1, KPNA2, RPS6*
Endoplasmic reticulum	$5.15\ e^{-4}$	0.032	*CYP51, HMOX1, LAMB2, ASPHD1, YIPF5, BST1, RDH10, SPTLC3, FAS, KIF1C, FKBP10, IFRG15, EXT2*
Regulation of leukocyte migration	$7.40\ e^{-4}$	0.033	*HMOX1, ADA, THBS1*
Transforming growth factor β binding	$8.56\ e^{-4}$	0.034	*THBS1, TGFBR2*
Homeostasis of number of cells	$8.44\ e^{-4}$	0.034	*LYN, JMJD6, HMOX1, RPS6*
Signal transmission via phosphorylation event	$1.16\ e^{-3}$	0.038	*EGFR, DBNL, THBS1, TNIK, STK17A, HMOX1, TNFRSF10B*
Regulation of nuclear mRNA spicing, via spliceosome	$1.47\ e^{-3}$	0.043	*JMJD3, CWC22*
Morphogenesis of an epithelial fold	$1.47\ e^{-3}$	0.043	*EGFR, RDH10*

defined the enriched GO terms, separately for proteins up-regulated and down-regulated in response to AngII. The enriched terms were then visualized by using the EM plugin (52), a tool for functional enrichment visualization, which minimized redundancy thus making results easier to interpret. Cellular response to AngII stimulation is visualized in Fig. 4*A*. Each *circle* in Fig. 4*A* represents a significantly enriched GO term, with *red color* indicating significance. The *inner circle* in Fig. 4*A* represents proteins up-regulated by AngII, and the *outer circle* represents those down-regulated. *Green edges* in Fig. 4*A* indicate that up-regulated proteins are shared by the two GO terms they connect, and *blue edges* indicate that down-regulated proteins are shared. Regulation of immune response, cell proliferation, and response to stress are enriched processes among the proteins up-regulated by AngII, although wound healing and regulation of cell migration are enriched among both up- and down-regulated proteins. Regulation of lipoprotein particle clearance was an enriched process among proteins significantly down-regulated by AngII (Fig. 4*B*), suggesting that AngII may play a direct role in regulating clearance of low density lipoproteins in PTECs.

We next used Ingenuity pathway analysis to assess the over-represented pathways among our 83 AngII-regulated proteins. The top five enriched canonical pathways included the following: mammalian target of rapamycin, p70S6K, phospholipase C, anti-proliferative role of TOB in T-cell signaling, and the super-pathway of cholesterol biosynthesis. Nrf2 oxidative stress pathway was also significantly enriched ($p = 0.039$). Protein networks with scores of ≥34 (equivalent to FDR ≤0.06%) included NFκB, PDGF, TGF, and ubiquitin-related networks (data not shown).

Systems Biology Approach to Analyzing the AngII Proteome—We next took advantage of the post-analysis feature in EM, which allows comparison of enriched GO terms between distinct groups of genes or proteins. We aimed to capture significant functional groups in our protein set that would be reproducible in a similar experiment performed in a different laboratory. Mice with global AT-1R knock-out (KO) and wild type (WT) mice were infused with AngII (53). The kidneys of these mice were then harvested, and gene expression was examined by microarray analysis. By taking the list of genes that were differentially expressed between the two groups of mice, and overlaying it on top of the EM presented in Fig. 4*A*, we generated Fig. 4*C*, which has one distant node containing significant genes from the mouse experiment. The *pink edges* in Fig. 4*C* represent overlap between the mouse gene set and the enriched gene sets from our experiment. Five GO terms were thus enriched in both gene sets as follows: regulation of response to stimulus; regulation of immune response; response to stress; organelle lumen; and membrane enclosed lumen. Genes responsible for significance of the term "response to stress" are shown in Fig. 4*C*. *Red arrows* in Fig. 4*C* point to genes in the Nrf2 pathway. *HMOX1* (encoding HO-1) is one of these genes and is common to all five enriched nodes shared between the two datasets. *HMOX1* was

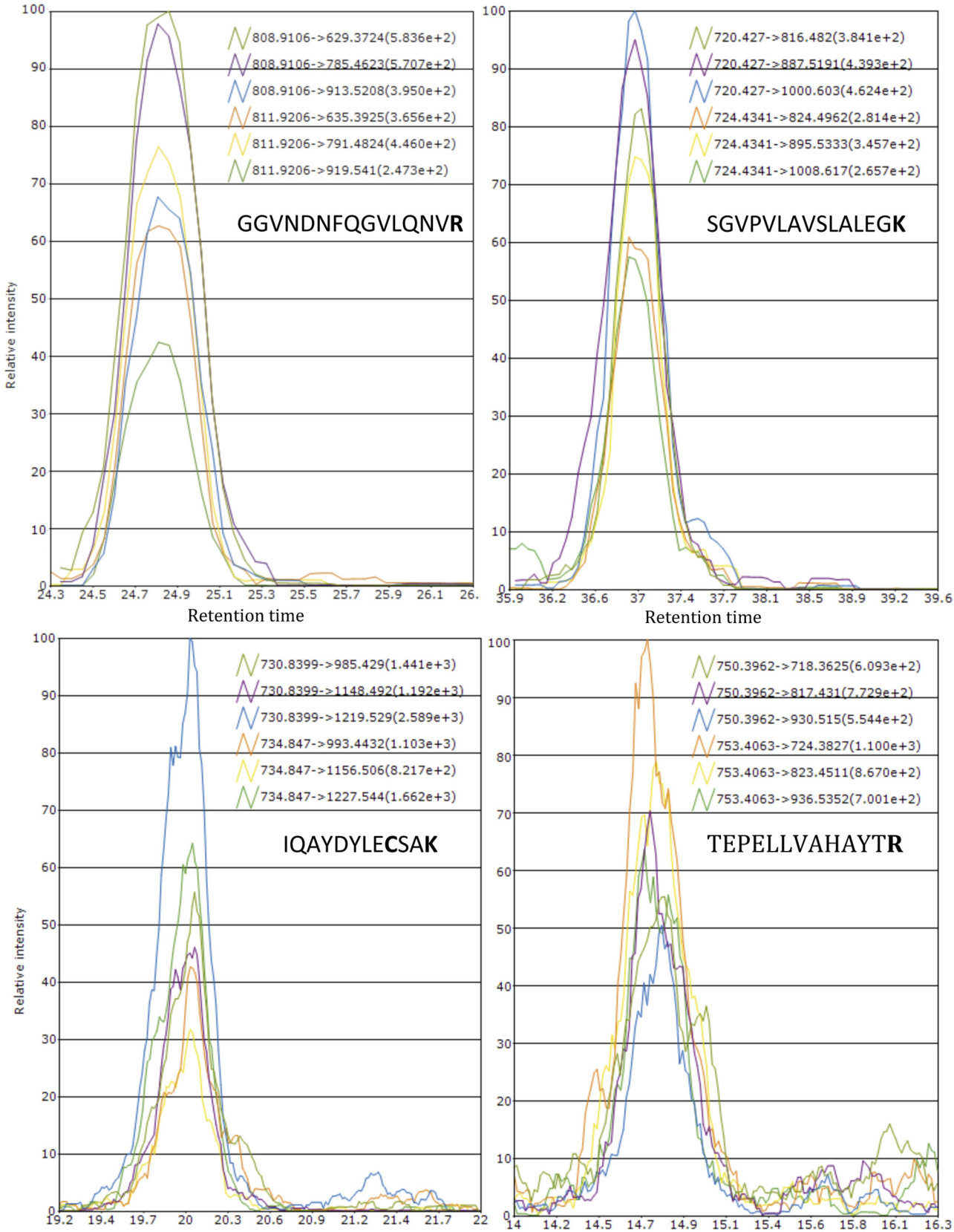

FIGURE 3. **Top three heavy and light transitions generated by Pinpoint to allow manual inspection and confirmation of heavy-to-light ratios.** *Top left panel,* TSP-1 peptide GGVNDNFQGVLQNVR; *top right panel,* PDCD4 peptide SGVPVLAVSLALEG**K**; *bottom left panel,* Rho-related GTP-binding protein peptide IQAYDYLE**C**SA**K**; and *bottom right panel*, HO-1 peptide TEPELLVAHAYT**R.** The top three transitions listed are light (control-treated), and the bottom three transitions are heavy (AngII-treated). Transition intensities are shown in *parentheses*.

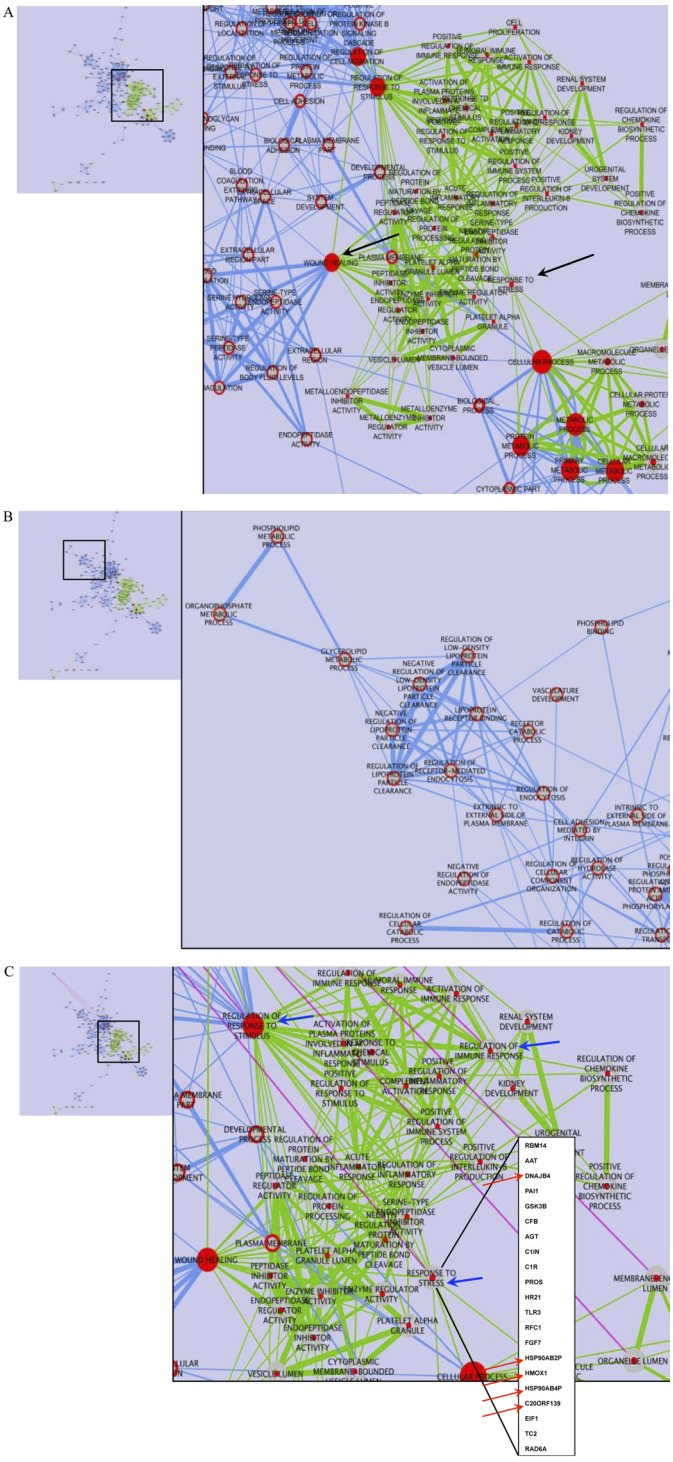

FIGURE 4. **EM of enriched GO terms among proteins differentially regulated by AngII in Cytoscape.** EM is depicted in the *left upper corner* of each image, with a *square* indicating the zoomed in area in the *right panel*. Each *circle* represents an enriched GO term, with *red color* indicating significance. The *inner circle* represents proteins up-regulated by AngII, whereas the *outer circle* represents those down-regulated. *Green edges* indicate that up-regulated proteins are shared by the two GO terms they connect, ands *blue edges* indicate that down-regulated proteins are shared. *A*, zoomed in image on the *right* demonstrates that response to stress is an enriched process in proteins up-regulated by AngII, whereas wound healing is enriched in both up- and down-regulated proteins. *B*, zoomed in on nodes significantly enriched among proteins down-regulated by AngII. Processes related to regulation of lipoprotein clearance are dominant. *C*, genes differentially regulated in kidneys of mice following AngII infusion are overlaid on top of the original EM in *A*. The *pink edges* represent overlap between the mouse gene set and the enriched gene sets from our experiment. Genes responsible for significance of the GO term response to stress are displayed. Five genes with *red arrows* pointing to them are in the Nrf2 pathway.

>8-fold up-regulated in WT compared with AT-1R KO mice following AngII infusion (53). The systems biology approach demonstrated that HO-1 protein and Nrf2 pathway are functionally important in response of the kidney to AngII.

Verification of HO-1 Protein and mRNA Up-regulation by AngII in PTECs—HO-1 was consistently up-regulated in the presence of AngII in our SILAC experiments, and it was one of the key proteins in our systems biology analysis. We thus proceeded to verify HO-1 protein up-regulation by ELISA in PTECs. PTECs were cultured to passage 6 in standard medium. They were then serum-deprived for 18 h and subsequently stimulated with AngII (10^{-7} M) or control for 8 h. AngII-stimulated cell lysates exhibited significantly higher HO-1 protein expression compared with controls ($p = 0.012$) (data not shown). We thus confirmed that AngII leads to up-regulation of HO-1 protein in primary PTECs.

We next examined whether HO-1 was regulated by AngII at the level of transcription by qRT-PCR. PTECs at passage 6 were serum-starved and then treated with control or AngII for 4 h. *HMOX1* was significantly up-regulated following AngII stimulation ($p = 0.018$) (data not shown). Two additional Nrf2-target genes were examined. *TXNIP* was significantly down-regulated by AngII treatment ($p = 0.025$) (data not shown), a result concordant with SILAC protein expression data. *DNAJB4* was not regulated at the level of transcription in AngII-treated PTECs ($p = 0.33$). These data suggest that AngII regulates HO-1 and thioredoxin-interacting protein mRNA levels either by influencing their transcription or affecting their stability.

In Vivo Studies of HO-1—Using a systems biology approach, we demonstrated that HO-1 up-regulation was likely AT-1R-dependent, and we verified AngII-mediated up-regulation of HO-1 in PTECs. We next examined whether HO-1 protein expression was increased following AngII infusion in the kidneys of mice with PTEC-specific AT-1R knock-out (PTKO), whether this increase was AT-1R-dependent, and finally, whether we could measure HO-1 in urine. Mice with AT-1R PTKO had been generated and characterized previously (27). AT-1R PTKO mice and control littermates (WT) were infused with AngII (1000 ng/kg/min) for 15 days. Immunohistochemistry of AngII-treated WT mouse kidneys demonstrated increased HO-1 expression in cortex relative to medulla (Fig. 5*A*). Intense cortical staining was observed predominantly in the proximal tubules (Fig. 5*B*). To quantify HO-1 expression, we performed Western blotting of kidney tissues. Blot images and densitometry are presented in Fig. 6*A*. WT mice showed a clear trend toward higher HO-1 renal expression levels compared with AT-1R PTKO mice ($p = 0.11$).

Finally, we evaluated urine HO-1 protein excretion in WT and AT-1R PTKO mice. Urine had been collected on day 13 of AngII infusion. *Box and whiskers plot* showing HO-1 urine protein excretion adjusted for urine creatinine is displayed in Fig. 6*B*. A clear separation between the two groups is depicted, with a trend toward higher HO-1 excretion in the WT compared with PTKO animals ($p = 0.12$). There was a positive linear

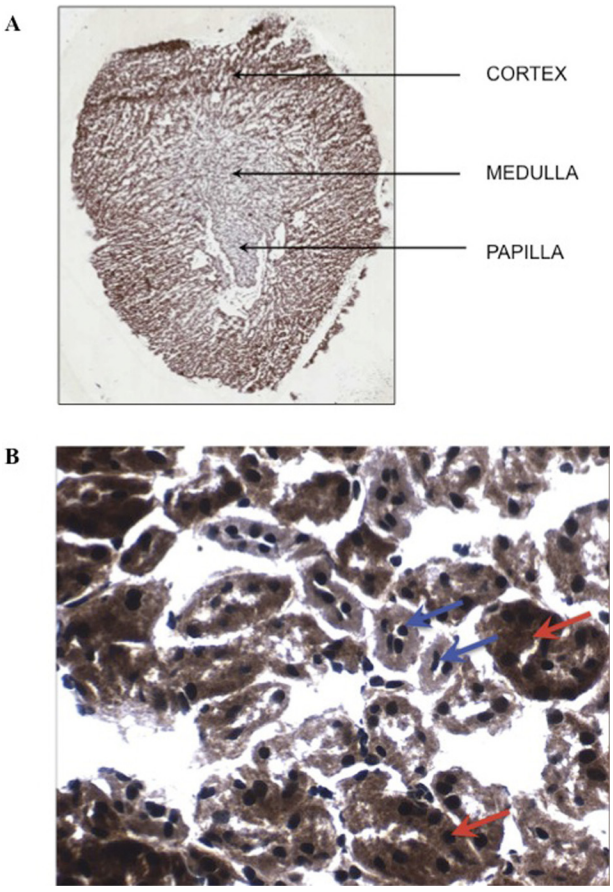

FIGURE 5. **HO-1 immunohistochemistry staining of kidneys from WT mice treated with AngII.** Representative fresh frozen sections are shown. *A,* cross-sectional view of the kidney at ×2 magnification. Increased cortical HO-1 staining relative to medulla is demonstrated. *B,* ×40 magnification; increased HO-1 staining is noted in proximal tubules (*red arrows*), whereas neighboring distal tubules (*blue arrows*) demonstrate less staining.

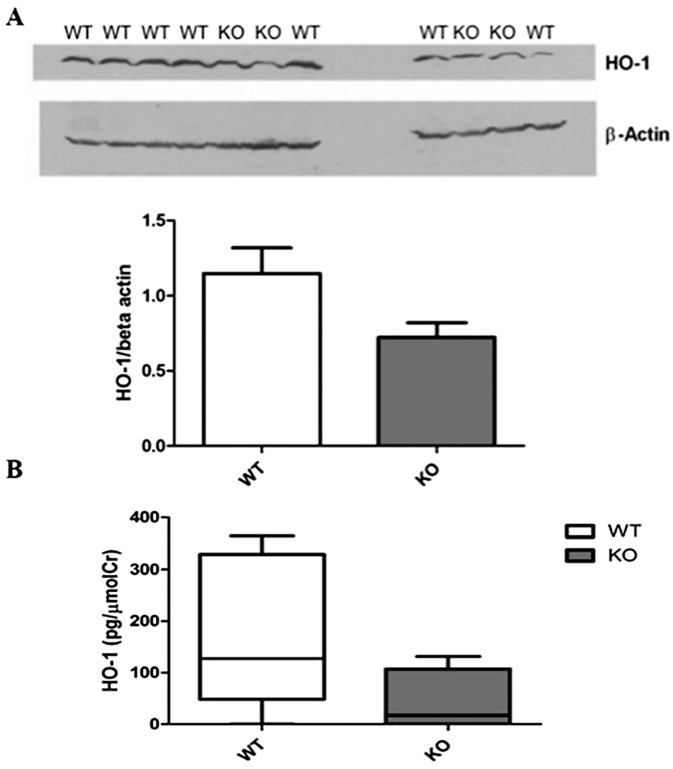

FIGURE 6. ***In vivo*** **quantification of HO-1 protein in mice with PTEC-specific AT-1R KO.** *A,* Western blotting for HO-1 in wild type mice (*WT*) and mice with PTEC-specific AT-1R knock out (*KO*) treated with a 15-day infusion of AngII. Densitometry readings for HO-1 adjusted for β-actin are represented as mean ± S.E. $p = 0.11$, difference between means = 0.43 ± 0.24 (95% confidence interval, −0.11, 0.97). *B,* urine HO-1 measurement by ELISA and adjusted for creatinine in WT and KO mice. *Horizontal lines* represent 1st, 2nd, and 3rd quartiles, and whiskers the range. $p = 0.12$, difference between means = 132.8 ± 78.2 (95% CI, −44.2, 309.7). Same 11 mice were used in both experiments.

correlation between tissue and urine HO-1 protein levels (Fig. 7), so that for every unit increase in tissue HO-1, there was a 194 pg/μmol creatinine increase in urine HO-1 ($p = 0.048$).

DISCUSSION

This study was designed to develop markers of AngII activity in the kidney. Our specific goal was to capture an "AngII protein signature" *in vitro* that reflected an early and consistent response of the PTEC to AngII. Three major aims of our study were as follows: 1) to define the proteome of AngII-stimulated PTECs; 2) to use systems biology to define the key biological processes mediated by AngII-regulated proteins; and 3) to extend *in vitro* observations in PTECs to *in vivo* observations in the kidney.

To address our first aim, we utilized SILAC methodology (35), which is the current standard for accurate relative quantification of entire cellular proteomes by mass spectrometry. We identified over 5000 proteins, most of which were also quantified, thus providing a unique depth of insight into PTEC responses to AngII. The strengths of our approach include excellent proteome coverage using extensive fractionation, instruments with high sensitivity and accuracy, multiple biological replicates and use of reverse labeling, and control experiments to minimize false-positive hits. Additionally, AngII-regulated proteome represents PTEC responses from three distinct individuals, thus signifying true biological variability, not typical of transformed cell culture models. To the best of our knowledge, this is the first effort to date to characterize proteomic responses of human kidney cells to AngII stimulation.

SILAC results for some AngII-regulated proteins were confirmed by SRM assay. Most of the proteins regulated by AngII were found at low abundance in PTECs. We thus selected 18 candidates, based on their convincing expression or their presence in biological processes of interest. All 18 of these had concordant relative expression when measured by SILAC and SRM, thus adding strength to our discovery approach.

To address our second aim, we used a systems biology approach to demonstrate biological processes fundamental in PTEC response to AngII. The dominant biological process identified among our 83 differentially regulated proteins was apoptosis, and the most enriched cellular compartment was ER. Furthermore, we demonstrated that response to stress and "wound healing" were some of the prominent AngII-driven biological processes. The common thread to these enriched GO terms is oxidative stress leading to ER stress and unfolded protein response, which could trigger apoptosis. The processes of apoptosis and oxidative stress were represented among the 18 proteins confirmed with SRM. The cascade leading from oxidative stress to apoptosis was indirectly linked to RAS in the kidney (54). AngII was previously shown to induce apoptosis in

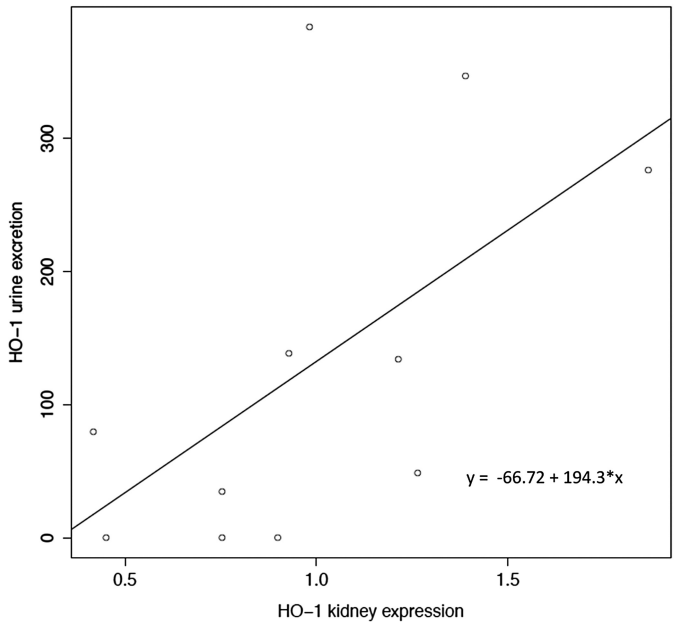

FIGURE 7. **Correlation between HO-1 kidney tissue expression (densitometry units of HO-1/β-actin) and HO-1 urine protein excretion (pg/μmol creatinine).** Linear regression line is displayed. $p = 0.048$; $\beta = 194.3$; 95% CI, 27.1, 361.5.

PTECs (55–57), as well as in other kidney cells (58, 59). The importance of our observations that apoptosis and oxidative stress dominate early PTEC responses to AngII is that we performed an unbiased search for differentially regulated proteins, which was not the case in any of the previously published studies. It may be of interest that processes involved in low density lipoprotein (LDL) clearance were enriched among proteins down-regulated by AngII. Kidney participates in the metabolism of lipoproteins (60) but is also a target of lipoprotein accumulation, which may participate in disease progression (60, 61). An increase in PTEC cholesterol content after acute kidney injury was deemed cytoprotective by maintaining plasma membrane integrity (62). Our work hints at the direct role AngII may have in impairing LDL clearance from renal tissue.

We next analyzed significant pathways and networks defined by our AngII-regulated proteins. The top canonical pathways and networks were congruent with prior understanding of AngII effects on the kidney, particularly its role in proliferation (63), hypertrophy (64), hypertension (65), inflammation (66, 67), and fibrosis (67–71).

We sought to validate our *in vitro* observations related to AngII-regulated proteins in an *in vivo* model using a systems biology approach. We examined which enriched functional groups of proteins from our experiment were also significant in a dataset of differentially expressed kidney genes from the AngII-infused WT mice and AT-1R KO mice. Five functional groups were common to both datasets, suggesting common and potentially fundamental findings across two experimental platforms. HO-1 was the most prominent individual protein regulated by AngII in our SILAC experiments, and it was also present in all five functional groups of genes. We thus verified HO-1 protein up-regulation in PTECs by ELISA, and HO-1 mRNA up-regulation by qRT-PCR. Prior studies support our observations related to HO-1. Nath and co-workers (72) first described HO-1 up-regulation in rat PTECs in response to AngII both *in vitro* and *in vivo* and demonstrated that heme-dependent stabilization of Nrf2 was responsible for HO-1 induction (73). AngII-induced HO-1 up-regulation was demonstrated *in vivo* in animal models of kidney disease by other groups (74–76). Increased renal immunostaining for HO-1 correlated with AngII and angiotensinogen immunostaining in biopsies of humans with IgA nephropathy (77). We believe that our study is the first to demonstrate HO-1 up-regulation by AngII in primary human kidney cells. Nrf2 target proteins appeared important based on direct SILAC data, and also based on bioinformatic analyses. Nrf2 is a transcription factor that becomes phosphorylated in the cytoplasm in response to oxidative stress, and it translocates to the nucleus, where it results in transcription of multiple genes responsible for reduction of oxidative damage, repair, and removal of damaged proteins, and activation of phase I–III-detoxifying proteins. HO-1, a key Nrf2-target protein, emerged as an important protein in cellular response to AngII based on our *in vitro* evidence and *in vivo* evidence from mice with global AT-1R KO.

Based on these observations, we went on to examine whether AngII effects in PTECs *in vitro* were relevant in mice with PTEC-specific AT-1R KO *in vivo*. These mice were chosen because they fully recapitulated our *in vitro* model and because they enabled us to test whether at least some of the effects of AngII were AT-1R-dependent. In addressing our third aim, we demonstrated that mice with AT-1R PTKO had a trend toward lower HO-1 kidney protein expression, suggesting that AngII up-regulates HO-1 in mouse kidneys via AT-1R and that PTECs contribute substantially to kidney HO-1 content. The literature suggests that HO-1 is only weakly expressed in the healthy kidney, and its expression is localized to proximal and distal tubules, the loop of Henle, and medullary collecting tubules (78). Upon injury, HO-1 is up-regulated in the tubules. Despite this broad tubular expression of HO-1, we found a trend in difference in HO-1 expression between AT-1R PTKO and WT mice following AngII infusion even when genetic manipulation was limited to proximal tubules. Moreover, AT-1R gene deletion with Cre recombinase resulted in only 50% reduction in gene expression, which likely also accounted for the lack of significance in HO-1 expression between the two mouse groups. We suggest that AT-1R was responsible for AngII-mediated HO-1 induction. Several other studies have corroborated this observation (74, 76, 79).

Our final aim was to relate differences in tissue expression to changes in urine excretion. We demonstrated that HO-1 protein was measurable in urine of mice during AngII infusion and displayed a trend toward lower excretion in animals with AT-1R PTKO compared with WT mice, which was paralleled by the findings in kidneys of these same animals. HO-1 protein excretion in urine is low or undetectable in normal humans and mice, but it was increased in humans and animals with acute kidney injury (80), another setting where RAS activation may contribute to kidney injury.[5] HO-1 protein expression was also

[5] F. Fang, G. C. Liu, X. Zhou, S. Yang, H. N. Reich, V. Williams, A. Hu, J. Pan, A. Konvalinka, G. Y. Oudit, J. W. Scholey, and R. John, submitted for publication.

increased in tubular cells isolated from the urine of patients with tubulointerstitial disorders (81). Finally, we found a direct linear relationship between kidney HO-1 protein expression and urine HO-1 excretion, suggesting that HO-1 excreted in urine is determined by its renal production. These findings suggest that novel markers of RAS activity in PTECs of the kidney can be measured in urine.

The literature addressing markers of RAS activity in the kidney has focused primarily on measuring urine excretion rates of angiotensinogen. Angiotensinogen is a precursor protein that is enzymatically cleaved by renin to generate angiotensin I, which is subsequently cleaved by angiotensin-converting enzyme to generate AngII. Several studies have reported increased urinary angiotensinogen excretion in patients with CKD, and in a few studies angiotensinogen excretion correlated with CKD progression (82–88). The rationale for measuring substrate levels is that the plasma angiotensinogen level is poised near the K_m values for cleavage by renin, with the consequence that alteration of angiotensinogen levels also affects the formation of AngII (89). Nonetheless, intra-renal RAS is complex, and substrate measurements likely do not represent the true degree of RAS bioactivity (90). We provide the first evidence of "AngII signature proteins" differentially expressed by PTECs, which could prove useful as markers of AngII activity in the kidney.

Despite our novel findings, our study has several limitations. Most significantly, we studied PTEC responses to AngII at a single time point, and the expression levels of proteins are likely to be dynamic rather than static. Although we studied a single time point, the variety of processes detected have been implicated in AngII-related and CKD processes. The secretome analysis was limited to a single replicate and thus could contribute only marginally to the overall findings. Some proteins were not amenable to SRM quantification due to their low expression levels in PTECs. Finally, our study was limited by the availability of kidney tissue and urine samples from mice with AT-1R PTKO.

In conclusion, we present the first study of human primary PTEC responses to AngII. We identified and confirmed 18 AngII signature proteins, which revealed biological processes of AngII activity. HO-1 emerged as the top AngII-regulated candidate in our *in vitro* and systems biology approaches. HO-1 was also regulated by AngII *in vivo*, and this was reflected in urinary measurements. These findings suggest that AngII signature proteins measured in urine may represent markers of AngII bioactivity in the kidney in patients and in experimental models.

REFERENCES

1. Wolf, G., and Ziyadeh, F. N. (1997) The role of angiotensin II in diabetic nephropathy: emphasis on nonhemodynamic mechanisms. *Am. J. Kidney Dis.* **29,** 153–163
2. Knight, S. F., and Imig, J. D. (2007) Obesity, insulin resistance, and renal function. *Microcirculation* **14,** 349–362
3. Lewis, E. J., Hunsicker, L. G., Bain, R. P., and Rohde, R. D. (1993) The effect of angiotensin-converting-enzyme inhibition on diabetic nephropathy. The Collaborative Study Group. *N. Engl. J. Med.* **329,** 1456–1462
4. Lewis, E. J., Hunsicker, L. G., Clarke, W. R., Berl, T., Pohl, M. A., Lewis, J. B., Ritz, E., Atkins, R. C., Rohde, R., and Raz, I. (2001) Renoprotective effect of the angiotensin-receptor antagonist irbesartan in patients with nephropathy due to type 2 diabetes. *N. Engl. J. Med.* **345,** 851–860
5. Wolf, G., and Ritz, E. (2005) Combination therapy with ACE inhibitors and angiotensin II receptor blockers to halt progression of chronic renal disease: pathophysiology and indications. *Kidney Int.* **67,** 799–812
6. Brenner, B. M., Cooper, M. E., de Zeeuw, D., Keane, W. F., Mitch, W. E., Parving, H. H., Remuzzi, G., Snapinn, S. M., Zhang, Z., and Shahinfar, S. (2001) Effects of losartan on renal and cardiovascular outcomes in patients with type 2 diabetes and nephropathy. *N. Engl. J. Med.* **345,** 861–869
7. Kunz, R., Friedrich, C., Wolbers, M., and Mann, J. F. (2008) Meta-analysis: effect of monotherapy and combination therapy with inhibitors of the renin angiotensin system on proteinuria in renal disease. *Ann. Intern. Med.* **148,** 30–48
8. Laverman, G. D., Navis, G., Henning, R. H., de Jong, P. E., and de Zeeuw, D. (2002) Dual renin-angiotensin system blockade at optimal doses for proteinuria. *Kidney Int.* **62,** 1020–1025
9. Russo, D., Pisani, A., Balletta, M. M., De Nicola, L., Savino, F. A., Andreucci, M., and Minutolo, R. (1999) Additive antiproteinuric effect of converting enzyme inhibitor and losartan in normotensive patients with IgA nephropathy. *Am. J. Kidney Dis.* **33,** 851–856
10. Mann, J. F., Schmieder, R. E., McQueen, M., Dyal, L., Schumacher, H., Pogue, J., Wang, X., Maggioni, A., Budaj, A., Chaithiraphan, S., Dickstein, K., Keltai, M., Metsärinne, K., Oto, A., Parkhomenko, A., Piegas, L. S., Svendsen, T. L., Teo, K. K., Yusuf, S., and ONTARGET investigators (2008) Renal outcomes with telmisartan, ramipril, or both, in people at high vascular risk (the ONTARGET study): a multicentre, randomised, double-blind, controlled trial. *Lancet* **372,** 547–553
11. Parving, H. H., Brenner, B. M., McMurray, J. J., de Zeeuw, D., Haffner, S. M., Solomon, S. D., Chaturvedi, N., Persson, F., Desai, A. S., Nicolaides, M., Richard, A., Xiang, Z., Brunel, P., and Pfeffer, M. A. (2012) Cardiorenal end points in a trial of Aliskiren for type 2 diabetes. *N. Engl. J. Med.* **367,** 2204–2213
12. Zimmerman, J. B., Robertson, D., and Jackson, E. K. (1987) Angiotensin II-noradrenergic interactions in renovascular hypertensive rats. *J. Clin. Invest.* **80,** 443–457
13. Purdy, R. E., and Weber, M. A. (1988) Angiotensin II amplification of α-adrenergic vasoconstriction: role of receptor reserve. *Circ. Res.* **63,** 748–757
14. Wilcox, C. S., Welch, W. J., and Snellen, H. (1991) Thromboxane mediates renal hemodynamic response to infused angiotensin II. *Kidney Int.* **40,** 1090–1097
15. Wagner, C., Jensen, B. L., Krämer, B. K., and Kurtz, A. (1998) Control of the renal renin system by local factors. *Kidney Int. Suppl.* **67,** S78–S83
16. Dzau, V. J. (1993) Tissue renin-angiotensin system in myocardial hypertrophy and failure. *Arch. Intern. Med.* **153,** 937–942
17. Kifor, I., Moore, T. J., Fallo, F., Sperling, E., Chiou, C. Y., Menachery, A., and Williams, G. H. (1991) Potassium-stimulated angiotensin release from superfused adrenal capsules and enzymatically dispersed cells of the zona glomerulosa. *Endocrinology* **129,** 823–831
18. Naftilan, A. J., Zuo, W. M., Inglefinger, J., Ryan, T. J., Jr., Pratt, R. E., and Dzau, V. J. (1991) Localization and differential regulation of angiotensinogen mRNA expression in the vessel wall. *J. Clin. Invest.* **87,** 1300–1311
19. Ingelfinger, J. R., Zuo, W. M., Fon, E. A., Ellison, K. E., and Dzau, V. J. (1990) *In situ* hybridization evidence for angiotensinogen messenger RNA in the rat proximal tubule. An hypothesis for the intrarenal renin angiotensin system. *J. Clin. Invest.* **85,** 417–423
20. Seikaly, M. G., Arant, B. S., Jr., and Seney, F. D., Jr. (1990) Endogenous angiotensin concentrations in specific intrarenal fluid compartments of the rat. *J. Clin. Invest.* **86,** 1352–1357
21. Kobori, H., Nangaku, M., Navar, L. G., and Nishiyama, A. (2007) The intrarenal renin-angiotensin system: from physiology to the pathobiology of hypertension and kidney disease. *Pharmacol. Rev.* **59,** 251–287
22. Navar, L. G., and Nishiyama, A. (2004) Why are angiotensin concentrations so high in the kidney? *Curr. Opin. Nephrol. Hypertens* **13,** 107–115
23. Siragy, H. M., and Carey, R. M. (2010) Role of the intrarenal renin-angiotensin-aldosterone system in chronic kidney disease. *Am. J. Nephrol.* **31,** 541–550
24. Bader, M., and Ganten, D. (2008) Update on tissue renin-angiotensin systems. *J. Mol. Med.* **86,** 615–621
25. Imig, J. D., Navar, G. L., Zou, L. X., O'Reilly, K. C., Allen, P. L., Kaysen, J. H.,

Hammond, T. G., and Navar, L. G. (1999) Renal endosomes contain angiotensin peptides, converting enzyme, and AT(1A) receptors. *Am. J. Physiol.* **277,** F303–F311
26. Zhuo, J. L., Imig, J. D., Hammond, T. G., Orengo, S., Benes, E., and Navar, L. G. (2002) AngII accumulation in rat renal endosomes during AngII-induced hypertension: role of AT(1) receptor. *Hypertension* **39,** 116–121
27. Gurley, S. B., Riquier-Brison, A. D., Schnermann, J., Sparks, M. A., Allen, A. M., Haase, V. H., Snouwaert, J. N., Le, T. H., McDonough, A. A., Koller, B. H., and Coffman, T. M. (2011) AT1A angiotensin receptors in the renal proximal tubule regulate blood pressure. *Cell Metab.* **13,** 469–475
28. Zhuo, J. L., and Li, X. C. (2007) Novel roles of intracrine angiotensin II and signalling mechanisms in kidney cells. *J. Renin Angiotensin Aldosterone Syst.* **8,** 23–33
29. Johnston, C. I. (1992) Franz Volhard Lecture. Renin-angiotensin system: a dual tissue and hormonal system for cardiovascular control. *J. Hypertens. Suppl.* **10,** S13–26
30. Dzau, V. J. (2001) Theodore Cooper Lecture: Tissue angiotensin and pathobiology of vascular disease: a unifying hypothesis. *Hypertension* **37,** 1047–1052
31. Mendelsohn, F. A. (1982) Angiotensin II: evidence for its role as an intrarenal hormone. *Kidney Int. Suppl.* **12,** S78–81
32. Tang, S. S., Jung, F., Diamant, D., Brown, D., Bachinsky, D., Hellman, P., and Ingelfinger, J. R. (1995) Temperature-sensitive SV40 immortalized rat proximal tubule cell line has functional renin-angiotensin system. *Am. J. Physiol.* **268,** F435–F446
33. Ingelfinger, J. R., Jung, F., Diamant, D., Haveran, L., Lee, E., Brem, A., and Tang, S. S. (1999) Rat proximal tubule cell line transformed with origin-defective SV40 DNA: autocrine ANG II feedback. *Am. J. Physiol.* **276,** F218–F227
34. Harrison-Bernard, L. M., Zhuo, J., Kobori, H., Ohishi, M., and Navar, L. G. (2002) Intrarenal AT(1) receptor and ACE binding in ANG II-induced hypertensive rats. *Am. J. Physiol. Renal Physiol.* **282,** F19–F25
35. Ong, S. E., Blagoev, B., Kratchmarova, I., Kristensen, D. B., Steen, H., Pandey, A., and Mann, M. (2002) Stable isotope labeling by amino acids in cell culture, SILAC, as a simple and accurate approach to expression proteomics. *Mol. Cell. Proteomics* **1,** 376–386
36. Makawita, S., Smith, C., Batruch, I., Zheng, Y., Ruckert, F., Grutzmann, R., Pilarsky, C., Gallinger, S., and Diamandis, E. P. (2011) Integrated proteomic profiling of cell line conditioned media and pancreatic juice for the identification of pancreatic cancer biomarkers. *Mol. Cell. Proteomics* **10,** M111 008599
37. Cox, J., and Mann, M. (2008) MaxQuant enables high peptide identification rates, individualized p.p.b.-range mass accuracies and proteome-wide protein quantification. *Nat. Biotechnol.* **26,** 1367–1372
38. MacLean, B., Tomazela, D. M., Shulman, N., Chambers, M., Finney, G. L., Frewen, B., Kern, R., Tabb, D. L., Liebler, D. C., and MacCoss, M. J. (2010) Skyline: an open source document editor for creating and analyzing targeted proteomics experiments. *Bioinformatics* **26,** 966–968
39. Drabovich, A. P., Jarvi, K., and Diamandis, E. P. (2011) Verification of male infertility biomarkers in seminal plasma by multiplex selected reaction monitoring assay. *Mol. Cell. Proteomics* **10,** M110 004127
40. Drabovich, A. P., and Diamandis, E. P. (2010) Combinatorial peptide libraries facilitate development of multiple reaction monitoring assays for low abundance proteins. *J. Proteome Res.* **9,** 1236–1245
41. Drabovich, A. P., Pavlou, M. P., Dimitromanolakis, A., and Diamandis, E. P. (2012) Quantitative analysis of energy metabolic pathways in MCF-7 breast cancer cells by selected reaction monitoring assay. *Mol. Cell. Proteomics* **11,** 422–434
42. Maclean, B., Tomazela, D. M., Abbatiello, S. E., Zhang, S., Whiteaker, J. R., Paulovich, A. G., Carr, S. A., and Maccoss, M. J. (2010) Effect of collision energy optimization on the measurement of peptides by selected reaction monitoring (SRM) mass spectrometry. *Anal. Chem.* **82,** 10116–10124
43. Maere, S., Heymans, K., and Kuiper, M. (2005) BiNGO: a Cytoscape plugin to assess overrepresentation of gene ontology categories in biological networks. *Bioinformatics* **21,** 3448–3449
44. Cline, M. S., Smoot, M., Cerami, E., Kuchinsky, A., Landys, N., Workman, C., Christmas, R., Avila-Campilo, I., Creech, M., Gross, B., Hanspers, K., Isserlin, R., Kelley, R., Killcoyne, S., Lotia, S., Maere, S., Morris, J., Ono, K., Pavlovic, V., Pico, A. R., Vailaya, A., Wang, P. L., Adler, A., Conklin, B. R., Hood, L., Kuiper, M., Sander, C., Schmulevich, I., Schwikowski, B., Warner, G. J., Ideker, T., and Bader, G. D. (2007) Integration of biological networks and gene expression data using Cytoscape. *Nat. Protoc.* **2,** 2366–2382
45. Liu, G. C., Oudit, G. Y., Fang, F., Zhou, J., and Scholey, J. W. (2012) Angiotensin-(1–7)-induced activation of ERK1/2 is cAMP/protein kinase A-dependent in glomerular mesangial cells. *Am. J. Physiol. Renal Physiol.* **302,** F784–F790
46. Oudit, G. Y., Liu, G. C., Zhong, J., Basu, R., Chow, F. L., Zhou, J., Loibner, H., Janzek, E., Schuster, M., Penninger, J. M., Herzenberg, A. M., Kassiri, Z., and Scholey, J. W. (2010) Human recombinant ACE2 reduces the progression of diabetic nephropathy. *Diabetes* **59,** 529–538
47. Taussky, H. H. (1954) A microcolorimetric determination of creatine in urine by the Jaffe reaction. *J. Biol. Chem.* **208,** 853–861
48. Rankin, E. B., Tomaszewski, J. E., and Haase, V. H. (2006) Renal cyst development in mice with conditional inactivation of the von Hippel-Lindau tumor suppressor. *Cancer Res.* **66,** 2576–2583
49. Rangasamy, T., Cho, C. Y., Thimmulappa, R. K., Zhen, L., Srisuma, S. S., Kensler, T. W., Yamamoto, M., Petrache, I., Tuder, R. M., and Biswal, S. (2004) Genetic ablation of Nrf2 enhances susceptibility to cigarette smoke-induced emphysema in mice. *J. Clin. Invest.* **114,** 1248–1259
50. He, X., and Ma, Q. (2012) Redox regulation by nuclear factor erythroid 2-related factor 2: gatekeeping for the basal and diabetes-induced expression of thioredoxin-interacting protein. *Mol. Pharmacol.* **82,** 887–897
51. Zhang, J., Dinh, T. N., Kappeler, K., Tsaprailis, G., and Chen, Q. M. (2012) La autoantigen mediates oxidant induced de novo Nrf2 protein translation. *Mol. Cell. Proteomics* **11,** M111.015032
52. Merico, D., Isserlin, R., Stueker, O., Emili, A., and Bader, G. D. (2010) Enrichment map: a network-based method for gene-set enrichment visualization and interpretation. *PLoS One* **5,** e13984
53. Makhanova, N. A., Crowley, S. D., Griffiths, R. C., and Coffman, T. M. (2010) Gene expression profiles linked to AT1 angiotensin receptors in the kidney. *Physiol. Genomics* **42A,** 211–218
54. Aminzadeh, M. A., Sato, T., and Vaziri, N. D. (2012) Participation of endoplasmic reticulum stress in the pathogenesis of spontaneous glomerulosclerosis–role of intra-renal angiotensin system. *Transl. Res.* **160,** 309–318
55. Bhaskaran, M., Reddy, K., Radhakrishanan, N., Franki, N., Ding, G., and Singhal, P. C. (2003) Angiotensin II induces apoptosis in renal proximal tubular cells. *Am. J. Physiol. Renal Physiol.* **284,** F955–F965
56. Weidekamm, C., Hauser, P., Hansmann, C., Schwarz, C., Klingler, H., Mayer, G., and Oberbauer, R. (2002) Effects of AT1 and AT2 receptor blockade on angiotensin II-induced apoptosis of human renal proximal tubular epithelial cells. *Wien Klin. Wochenschr.* **114,** 725–729
57. Liu, F., Brezniceanu, M. L., Wei, C. C., Chénier, I., Sachetelli, S., Zhang, S. L., Filep, J. G., Ingelfinger, J. R., and Chan, J. S. (2008) Overexpression of angiotensinogen increases tubular apoptosis in diabetes. *J. Am. Soc. Nephrol.* **19,** 269–280
58. Lodha, S., Dani, D., Mehta, R., Bhaskaran, M., Reddy, K., Ding, G., and Singhal, P. C. (2002) Angiotensin II-induced mesangial cell apoptosis: role of oxidative stress. *Mol. Med.* **8,** 830–840
59. Susztak, K., Raff, A. C., Schiffer, M., and Böttinger, E. P. (2006) Glucose-induced reactive oxygen species cause apoptosis of podocytes and podocyte depletion at the onset of diabetic nephropathy. *Diabetes* **55,** 225–233
60. Reblin, T., Donarski, N., Fineder, L., Bräsen, J. H., Dieplinger, H., Thaiss, F., Stahl, R. A., Beisiegel, U., and Wolf, G. (2001) Renal handling of human apolipoprotein(a) and its fragments in the rat. *Am. J. Kidney Dis.* **38,** 619–630
61. Wanner, C., Greiber, S., Krämer-Guth, A., Heinloth, A., and Galle, J. (1997) Lipids and progression of renal disease: role of modified low density lipoprotein and lipoprotein (a). *Kidney Int. Suppl.* **63,** S102–106
62. Zager, R. A., Burkhart, K. M., Johnson, A. C., and Sacks, B. M. (1999) Increased proximal tubular cholesterol content: implications for cell injury and "acquired cytoresistance". *Kidney Int.* **56,** 1788–1797
63. Schelling, P., Fischer, H., and Ganten, D. (1991) Angiotensin and cell growth: a link to cardiovascular hypertrophy? *J. Hypertens.* **9,** 3–15
64. Wolf, G., and Neilson, E. G. (1990) Angiotensin II induces cellular hyper-

trophy in cultured murine proximal tubular cells. *Am. J. Physiol.* **259,** F768–F777
65. Kim, J. A., Jang, H. J., Martinez-Lemus, L. A., and Sowers, J. R. (2012) Activation of mTOR/p70S6 kinase by ANG II inhibits insulin-stimulated endothelial nitric oxide synthase and vasodilation. *Am. J. Physiol. Endocrinol. Metab.* **302,** E201–E208
66. Muller, D. N., Shagdarsuren, E., Park, J. K., Dechend, R., Mervaala, E., Hampich, F., Fiebeler, A., Ju, X., Finckenberg, P., Theuer, J., Viedt, C., Kreuzer, J., Heidecke, H., Haller, H., Zenke, M., and Luft, F. C. (2002) Immunosuppressive treatment protects against angiotensin II-induced renal damage. *Am. J. Pathol.* **161,** 1679–1693
67. Ruiz-Ortega, M., Rupérez, M., Esteban, V., Rodríguez-Vita, J., Sánchez-López, E., Carvajal, G., and Egido, J. (2006) Angiotensin II: a key factor in the inflammatory and fibrotic response in kidney diseases. *Nephrol. Dial. Transplant.* **21,** 16–20
68. Finckenberg, P., Inkinen, K., Ahonen, J., Merasto, S., Louhelainen, M., Vapaatalo, H., Müller, D., Ganten, D., Luft, F., and Mervaala, E. (2003) Angiotensin II induces connective tissue growth factor gene expression via calcineurin-dependent pathways. *Am. J. Pathol.* **163,** 355–366
69. Lautrette, A., Li, S., Alili, R., Sunnarborg, S. W., Burtin, M., Lee, D. C., Friedlander, G., and Terzi, F. (2005) Angiotensin II and EGF receptor cross-talk in chronic kidney diseases: a new therapeutic approach. *Nat. Med.* **11,** 867–874
70. Carvajal, G., Rodríguez-Vita, J., Rodrigues-Díez, R., Sánchez-López, E., Rupérez, M., Cartier, C., Esteban, V., Ortiz, A., Egido, J., Mezzano, S. A., and Ruiz-Ortega, M. (2008) Angiotensin II activates the Smad pathway during epithelial mesenchymal transdifferentiation. *Kidney Int.* **74,** 585–595
71. Yang, F., Chung, A. C., Huang, X. R., and Lan, H. Y. (2009) Angiotensin II induces connective tissue growth factor and collagen I expression via transforming growth factor-β-dependent and -independent Smad pathways: the role of Smad3. *Hypertension* **54,** 877–884
72. Haugen, E. N., Croatt, A. J., and Nath, K. A. (2000) Angiotensin II induces renal oxidant stress *in vivo* and heme oxygenase-1 *in vivo* and *in vitro*. *Kidney Int.* **58,** 144–152
73. Alam, J., Killeen, E., Gong, P., Naquin, R., Hu, B., Stewart, D., Ingelfinger, J. R., and Nath, K. A. (2003) Heme activates the heme oxygenase-1 gene in renal epithelial cells by stabilizing Nrf2. *Am. J. Physiol. Renal Physiol.* **284,** F743–F752
74. Aizawa, T., Ishizaka, N., Taguchi Ji., Nagai, R., Mori, I., Tang, S. S., Ingelfinger, J. R., and Ohno, M. (2000) Heme oxygenase-1 is up-regulated in the kidney of angiotensin II-induced hypertensive rats: possible role in renoprotection. *Hypertension* **35,** 800–806
75. Aizawa, T., Ishizaka, N., Kurokawa, K., Nagai, R., Nakajima, H., Taguchi, J., and Ohno, M. (2001) Different effects of angiotensin II and catecholamine on renal cell apoptosis and proliferation in rats. *Kidney Int.* **59,** 645–653
76. Ohashi, N., Katsurada, A., Miyata, K., Satou, R., Saito, T., Urushihara, M., and Kobori, H. (2009) Role of activated intrarenal reactive oxygen species and renin-angiotensin system in IgA nephropathy model mice. *Clin. Exp. Pharmacol. Physiol.* **36,** 750–755
77. Kobori, H., Katsurada, A., Ozawa, Y., Satou, R., Miyata, K., Hase, N., Suzaki, Y., and Shoji, T. (2007) Enhanced intrarenal oxidative stress and angiotensinogen in IgA nephropathy patients. *Biochem. Biophys. Res. Commun.* **358,** 156–163
78. da Silva, J. L., Zand, B. A., Yang, L. M., Sabaawy, H. E., Lianos, E., and Abraham, N. G. (2001) Heme oxygenase isoform-specific expression and distribution in the rat kidney. *Kidney Int.* **59,** 1448–1457
79. Chang, S. Y., Chen, Y. W., Chenier, I., Tran Sle, M., and Zhang, S. L. (2011) Angiotensin II type II receptor deficiency accelerates the development of nephropathy in type I diabetes via oxidative stress and ACE2. *Exp. Diabetes Res.* **2011,** 521076
80. Zager, R. A., Johnson, A. C., and Becker, K. (2012) Plasma and urinary heme oxygenase-1 in AKI. *J. Am. Soc. Nephrol.* **23,** 1048–1057
81. Yokoyama, T., Shimizu, M., Ohta, K., Yuno, T., Okajima, M., Wada, T., Toma, T., Koizumi, S., and Yachie, A. (2011) Urinary heme oxygenase-1 as a sensitive indicator of tubulointerstitial inflammatory damage in various renal diseases. *Am. J. Nephrol.* **33,** 414–420
82. Reams, G., Villarreal, D., Wu, Z., and Bauer, J. H. (1994) Urinary angiotensin II: a marker of renal tissue activity? *Nephron* **67,** 450–458
83. Vos, P. F., Boer, P., Braam, B., and Koomans, H. A. (1994) The origin of urinary angiotensins in humans. *J. Am. Soc. Nephrol.* **5,** 215–223
84. Kobori, H., Harrison-Bernard, L. M., and Navar, L. G. (2002) Urinary excretion of angiotensinogen reflects intrarenal angiotensinogen production. *Kidney Int.* **61,** 579–585
85. Kobori, H., Nishiyama, A., Harrison-Bernard, L. M., and Navar, L. G. (2003) Urinary angiotensinogen as an indicator of intrarenal angiotensin status in hypertension. *Hypertension* **41,** 42–49
86. Yamamoto, T., Nakagawa, T., Suzuki, H., Ohashi, N., Fukasawa, H., Fujigaki, Y., Kato, A., Nakamura, Y., Suzuki, F., and Hishida, A. (2007) Urinary angiotensinogen as a marker of intrarenal angiotensin II activity associated with deterioration of renal function in patients with chronic kidney disease. *J. Am. Soc. Nephrol.* **18,** 1558–1565
87. Nishiyama, A., Konishi, Y., Ohashi, N., Morikawa, T., Urushihara, M., Maeda, I., Hamada, M., Kishida, M., Hitomi, H., Shirahashi, N., Kobori, H., and Imanishi, M. (2011) Urinary angiotensinogen reflects the activity of intrarenal renin-angiotensin system in patients with IgA nephropathy. *Nephrol. Dial. Transplant.* **26,** 170–177
88. Mills, K. T., Kobori, H., Hamm, L. L., Alper, A. B., Khan, I. E., Rahman, M., Navar, L. G., Liu, Y., Browne, G. M., Batuman, V., He, J., and Chen, J. (2012) Increased urinary excretion of angiotensinogen is associated with risk of chronic kidney disease. *Nephrol. Dial. Transplant.* **27,** 3176–3181
89. Lifton, R. P. (1995) Genetic determinants of human hypertension. *Proc. Natl. Acad. Sci. U.S.A.* **92,** 8545–8551
90. Matsusaka, T., Niimura, F., Shimizu, A., Pastan, I., Saito, A., Kobori, H., Nishiyama, A., and Ichikawa, I. (2012) Liver angiotensinogen is the primary source of renal angiotensin II. *J. Am. Soc. Nephrol.* **23,** 1181–1189
91. Vizcaíno, J. A., Côté, R. G., Csordas, A., Dianes, J. A., Fabregat, A., Foster, J. M., Griss, J., Alpi, E., Birim, M., Contell, J., O'Kelly, G., Schoenegger, A., Ovelleiro, D., Pérez-Riverol, Y., Reisinger, F., Ríos, D., Wang, R., and Hermjakob, H. (2013) The PRoteomics IDEntifications (PRIDE) database and associated tools: status in 2013. *Nucleic Acids Res.* **41,** D1063–D1069